JOURNAL OF GEOPHYSICAL RESEARCH, VOL. 103, NO. C4, PAGES 8045–8057, APRIL 15, 1998

ERS-1/2 orbit improvement using TOPEX/POSEIDON: The 2 cm challenge

P.-Y. Le Traon and F. Ogor

Collecte, Localisation, Satellites Space Oceanography Division, Ramonville Saint-Agne, France

Abstract. The ERS orbit error reduction method using TOPEX/POSEIDON (T/P) data as a reference [*Le Traon et al.*, 1995a] was applied to ERS-1 cycles from phases C, E, F, and G and to the first 16 cycles of the ERS-2 mission (phase A). T/P M-GDR (geophysical data record) (version C) and ERS-1/2 ocean product (OPR) data were used. ERS-1/2 orbits are the D-PAF (processing and archiving facility) orbits and, when necessary, ERS-1/2 altimetric corrections were updated to make the T/P and ERS-1/2 corrections homogeneous. The adjustment method has been refined, and formal error on the estimation is now calculated. The ERS-1/2 orbit error estimation is thus estimated to be precise to within about 2 cm root-mean-square (rms). E-E crossover differences are reduced from 12 to 17 cm to only 6.5 cm rms for all processed cycles. Similarly, the T/P-E crossover differences are reduced from 11 to 14 cm to only 7 cm rms. The adjusted D-PAF orbit error varies between 6 and 12 cm rms. The adjustment has also been performed for the Joint Gravity Model 3(JGM 3) orbits of ERS-1 phases C, E, and F. The rms difference between the corrected orbits for the D-PAF and JGM 3 orbits is only about 1 cm rms, while it is about 11 cm before T/P orbit error correction. This shows that the adjustment is almost insensitive to the initial ERS-1 orbit used. It also confirms the 2 cm precision of the method. We also do repeat-track analysis on the 35 day repeat cycles of ERS-1 phase C. The mean difference in sea level variance before and after orbit error correction is 34 cm^2 (D-PAF orbit) and 17 cm^2 (JGM 3 orbit). The corrected ERS-1 and T/P sea level variabilities, however, are in excellent agreement. The study thus shows that ERS-1/2 orbit error must be corrected before analyzing large-scale oceanic signals and combining ERS-1/2 with T/P data. The proposed method provides a very effective correction and thus significantly enhances the quality of ERS-1/2 data. Corresponding data sets will be distributed to the scientific community by Archiving, Validation, and Interpretation of Satellite Oceanographic Data (AVISO).

1. Introduction

Since the launch of TOPEX/POSEIDON (T/P) in August 1992, several altimetric satellites (T/P, ERS-1, and ERS-2) have been flying simultaneously. This is likely to recur in the future with the Geosat follow-on, Envisat, and Jason missions. While T/P, with its unprecedented accuracy, has provided a new picture of the ocean, it cannot observe the full spectrum of the sea level and oceanic circulation. At least one more mission is needed, in particular, to resolve the mesoscale oceanic circulation. The ERS satellites are thus an excellent complement for T/P sampling. They provide a good resolution of the mesoscale oceanic circulation [e.g., *Hernandez et al.*, 1995] while T/P provides the large-scale oceanic circulation. They also provide coverage at high latitudes.

Merging the different altimetric data sets will provide better mappings of sea level variation and the geoid (or more exactly the mean sea surface) [e.g., *Rapp et al.*, 1994; P. Mazzega et al., Maps of the mean sea surface and corresponding gravity anomalies from ERS-1 geodetic mission, submitted to the *Journal of Geophysical Research*, 1996]. Merging multisatellite data sets requires homogeneous, intercalibrated data sets. This means first that the same altimetric corrections should be used (same tidal models, same meteorological models for inverse barometer and dry tropospheric corrections, etc.) and that orbits should generally be calculated with the same geopotential model and with consistent reference systems. To obtain intercalibrated data sets, we recommend using the most precise altimetric missions (T/P, Jason) as a reference for the other altimetric missions. This method has been shown to provide very good results with ERS-1 [*Le Traon et al.*, 1995a, b; *Carnochan et al.*, 1995]. Although ERS-1/2 orbit accuracy has been significantly improved since these studies, T/P is still much more precise. The ERS-1/2 orbits are accurate to within about 7–10 cm [*Scharroo et al.*, 1994; *Massmann et al.*, 1997] while T/P accuracy is 2 cm [e.g., *Fu et al.*, 1994; *Tapley et al.*, 1996]. In addition, contrary to T/P, the altimetric data themselves are generally used in ERS-1/2 orbit determination.

The purpose of the paper is to demonstrate that T/P can dramatically improve ERS-1/2 orbit accuracy and that the technique proposed by *Le Traon et al.* [1995a] is very effective at providing homogeneous and intercalibrated altimetric data sets. The paper is organized as follows. The ERS orbit error reduction method is briefly described in section 2, and the accuracy of the fit is analyzed in section 3. The method is then applied to the ERS-1 35 day repeat cycle mission (phase C), the ERS-1 geodetic mission (phases E and F), the second ERS-1 35 day repeat cycle mission (phase G), and the first 16 cycles of the ERS-2 35 day repeat cycle mission (phase A).

Paper number 97JC01917.
0148-0227/98/97JC-01917$09.00

Results are discussed in section 4. Analysis of sea level variability is performed in section 5 to demonstrate the improvement in ERS-1/2 data accuracy. The main conclusions and perspectives are given in section 6.

2. ERS Orbit Error Reduction Method

The ERS orbit error reduction method is described in detail by *Le Traon et al.* [1995a] and is only summarized here. The method is based on global minimization of T/P-E and E-E crossover differences. T/P-E crossover differences give an estimate of the ERS orbit almost directly, leading to a "geometric" estimation of orbit error. Smoothing cubic spline functions [*Hayes*, 1974] are then used to obtain a continuous estimation of orbit error over time. E-E crossovers further constrain the solution; this is particularly useful at high latitudes where there are no T/P-E crossovers.

The cubic spline representation of the ERS orbit error $E(t)$ is given by

$$E(t) = \sum_{k=1}^{K+4} c_k N_k(t) \tag{1}$$

$N_k(t)$ is the so-called normalized third-degree B spline defined on knots l_k, l_{k+1}, l_{k+2}, l_{k+3}, and l_{k+4}. The ERS orbit error reduction therefore consists of determining the $K + 4$ coefficients c_k which minimize the function $F(c_1, c_2, \cdots, c_K)$

$$F = \sum_{i=1}^{N} w_i^2[dc(t_i) - E(t_i)]^2 + \sum_{j=1}^{M} w_j^2[E(t_{ja}) - E(t_{jd}) - d_j]^2 \tag{2}$$

where $dc(t_i)$ is the dual crossover difference (T/P-ERS) at crossover i, which provides a direct estimate of ERS orbit error $E(t_i)$; t_{ja}, t_{jd}, and d_j are the times of the ascending and descending arcs and the ERS-ERS crossover differences at crossover j, respectively; N is the number of T/P-E dual crossovers; M is the number of E-E crossovers; and w_i are the weights for each observation.

To avoid removing part of the oceanic signal in the adjustment, the method applied by *Le Traon et al.* [1995a, b] only used T/P-E and E-E crossovers with time differences below 5 days. The method has now been somewhat refined. For T/P-E crossovers the T/P sea surface height estimation is linearly interpolated from the two T/P cycles surrounding the ERS arc (the two T/P cycles are separated by 10 days, the T/P cycle duration). This provides an estimate of the sea surface height at the time of the ERS arc and minimizes the oceanic signal contribution in the T/P-E crossover differences. E-E crossovers with time differences of up to 10 days are now also used but with weights w_i depending linearly on time differences. Weights decrease by a factor of 2 from 0 to 10 days. This was derived from an analysis of E-E crossover differences since weights should be inversely proportional to the root-mean-square (rms) crossover differences. The weights for T/P-E crossovers correspond to the weights of E-E crossovers with no time differences. At latitudes over 66°, where there are no T/P-E crossovers, the E-E crossover weights are multiplied by 2 to better constrain the solution, as explained by *Le Traon et al.* [1995a]; see also the discussion in section 3. Note, however, that there is no downweighting for the larger number of crossovers at high latitudes. T/P-E and E-E crossovers in shallow regions (<200 m) are not used in the minimization.

The strategy for positioning the knots was also slightly modified. Two knots are initially placed at the first and last T/P-E crossovers on a given ERS arc. When the two knots are more than 10,000 km apart and there are more than 20 T/P-E crossovers on the arc, an extra knot is placed at the middle T/P-E crossover on the arc. If the two knots are less than 5000 km apart or if there are fewer than 10 T/P-E crossovers on the arc, the second knot is removed. This typically corresponds to 2500 knots in all for about 50,000 dual crossovers and 20,000 single ERS-1 crossovers for a full 35 day cycle.

3. Accuracy of ERS Orbit Error Estimation

The adjustment of ERS data using T/P as a reference was previously shown to provide a very good estimate of ERS orbit error. This was assessed through crossover and repeat-track analysis before and after orbit error correction [*Le Traon et al.*, 1995a, b]. For a more quantitative assessment the formal error on the estimation is now calculated. The formal error is derived from standard least squares theory, but the calculation is complicated by the spline representation. The ERS orbit error estimation consists of minimizing the function F. F can be written as $(A\mathbf{X}\text{-}B)\ (A\mathbf{X}\text{-}B)^T$, where $\mathbf{X}$ is the vector of unknowns, i.e., the spline coefficients c_k. The standard least squares solution is $\mathbf{X} = (A^TA)^{-1}A^TB$, and the covariance matrix of $\mathbf{X}$, Cov ($\mathbf{X}$) is given by Cov ($\mathbf{X}$) $= (A^TA)^{-1}\sigma^2$, where σ^2 is the least squares residual (F) after minimization.

To obtain the error on the orbit estimation $E(t)$ from the error on $\mathbf{X}$, the nondiagonal terms of Cov ($\mathbf{X}$) have to be taken into account

$$\langle E(t)^2 \rangle = \sum_{k=1}^{K+4} \sum_{k'=1}^{K+4} \langle c_k c_l \rangle N_k(t) N_l(t) \tag{3}$$

This implies calculating the inverse of the normal matrix A^TA and estimating the variance of the error on the orbit error estimation $\langle E(t)^2 \rangle$ for any given t, given (3). This represents the fitting error only, which depends on the number and position of spline knots and on the least squares residual. It will not include the error due to orbit or large-scale errors unresolved by the spline representation.

The error estimate was used to refine the strategy for choosing the position of spline knots (see section 3). Plate 1a shows the estimated formal error when only T/P-E crossovers are used in the adjustment. The error is below 3 cm for latitudes below 66° and can reach 5 cm at high latitudes. The Mediterranean is also not very well constrained because of its geometry. This confirms, nevertheless, the very good fit obtained with the T/P-E crossovers. When the E-E crossovers are used, the error decreases to less than 2 cm below 66° and to about 3 cm at higher latitudes and in the Mediterranean (Plate 1b). With the overweighting of E-E crossovers at high latitudes the error is much more uniform, but given the overweighting, the result is not really representative of the true accuracy.

4. Application

4.1. Data

The method was applied to (1) ERS-1 cycles 6–18 of the first 35 day repeat cycle mission (October 1992 to December 1993) (ERS-1 phase C), (2) the two ERS-1 168 day cycles (geodetic mission) (ERS-1 phases E and F) split into eight subcycles of

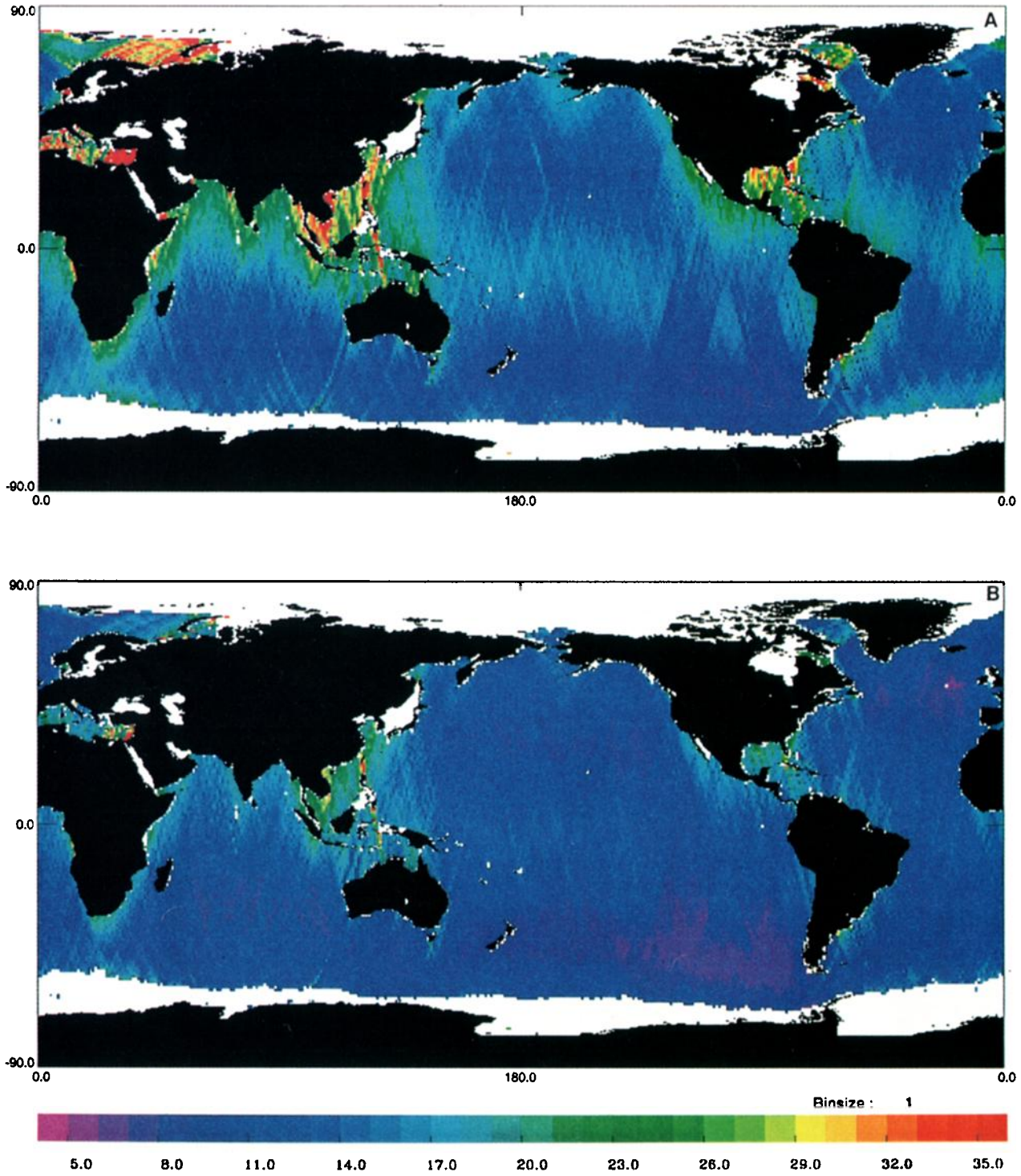

Plate 1. Formal error on ERS orbit error estimation (in centimeters) when (a) only TOPEX/POSEIDON (T/P)-E crossovers are used in the minimization and (b) when T/P-E and E-E crossovers are used in the minimization.

37 days and two subcycles of 20 days (April 1994 to March 1995), (3) ERS-1 cycles 1–13 of the second 35 day repeat cycle mission (March 1995 to June 1996) (ERS-1 phase G), and (4) ERS-2 cycles 1–16 (35 day repeat cycle mission) (May 1995 to November 1996) (ERS-2 phase A). T/P merged geophysical data records (GDR) distributed by Archiving, Validation, and Interpretation of Satellite Oceanographic Data (AVISO) [*AVISO*, 1996a] and ERS-1/2 ocean products (OPRs) distributed by Centre ERS d'Archivage et de Traitement (CERSAT) were used [*CERSAT*, 1994, 1996]. T/P data are the reprocessed merged GDRs (GDR-M, version C) [*AVISO*, 1996a]. They include the Center for Space Research (CSR) 3.0 tidal model [*Eanes et al.*, 1995], the National Aeronautics and Space Administration (NASA) and Centre National d'Etudes Spatiales (CNES) Joint Gravity Model 3(JGM 3) orbits [*Tapley et al.*, 1996; *Barotto and Berthias*, 1998], and a series of minor cor-

Table 1. TOPEX/POSEIDON and ERS-1/2 Data Sets Used for the Study

	TOPEX/POSEIDON	ERS
GDRs	GDR-M products, version C [*AVISO*, 1996a]	OPR products, version 3 for ERS-1 phases C, E, and F and version 6.2 for ERS-1 phase G and ERS-2 phase A [*CERSAT*, 1994, 1996]
Orbit	CNES JGM 3/ELFE orbits	D-PAF precise orbit referenced to TOPEX ellipsoid
Geophysical corrections		
Dry troposphere and inverse barometer effect	from ECMWF	from ECMWF, this is an upgrade for the ERS-1 version 3 products which used the ARPEGE model
Wet troposphere	from TMR radiometer	from ATSR-M radiometer[a]
Ionosphere	from dual-frequency altimeter range measurements for TOPEX data[b], from DORIS for POSEIDON data	BENT model
Sea state bias	BM4 [*Gaspar et al.*, 1994]	version 3, −5.5% of SWH [*Gaspar and Ogor*, 1994]; version 6.2, BM3 [*Gaspar and Ogor*, 1996] (update of the OPR)
Tides		
Ocean tide and loading tide	CSR3.0 [*Eanes and Bettadpur*, 1995]	CSR3.0 (update of the OPR)
Solid Earth tide	*Cartwright and Tayler* [1971]	*Cartwright and Tayler* [1971]
Pole tide	applied	not applied

[a]Corrected as indicated on the CLS ERS quality assessments [*CLS*, 1992, 1996a, b] and extrapolated near the coasts.
[b]Smoothed using a Lanczos filter (300 km).
TMR is TOPEX microwave radiometer, ATSR-M is along-track scanning radiometer-microwave, and DORIS is Doppler orbitography and radiopositioning integrated by satellite.

rections to the initial GDRs (e.g., sigma-0 calibration, polar tide correction). In addition, the TOPEX instrumental drift and bias were also corrected for. For ERS-1/2, D-PAF (processing and archiving facility) orbits were used [*Massmann et al.*, 1997]. When necessary, ERS-1/2 altimetric corrections were updated to make the T/P and ERS-1/2 corrections homogeneous. The CSR3.0 tidal model was thus used. The dry tropospheric and inverse barometer corrections, derived from the French meteorological model ARPEGE (until the end of the ERS-1 geodetic mission), were also replaced by corrections derived from the European Centre for Medium-Range Weather Forecasts (ECMWF) model as for T/P. The corrections applied to T/P and ERS-1/2 data are summarized in Table 1. ERS-1/2 altimeter biases, ultra stable oscillator (USO) drift, and single-point target response (SPTR) corrections were not applied since they can be fully corrected for by the orbit error reduction method. The same holds for the pole tide, which is not present in ERS-1/2 OPR. Finally, time tag biases of −1.3 and −1.1 ms were applied to ERS-1 and ERS-2 range measurements, respectively. The biases were derived from crossover analysis.

Given the very high constraint of the fit due to the very low T/P orbit error, the method should be almost insensitive to the initial orbit used. This was checked by also performing the adjustment for the Delft JGM 3 precise orbits [*Scharroo et al.*, 1994] for ERS-1 phases C, E, and F and comparing with the results obtained from D-PAF orbits.

4.2. Results

Figures 1 and 2 show the statistics of T/P-E and E-E crossovers for all processed cycles for the D-PAF and JGM 3 ERS-1 orbits (phases C, E, and F), for the D-PAF ERS-1 orbits (phase G), and for the D-PAF ERS-2 orbits (phase A). Before orbit error adjustment the E-E crossovers for time lags below 10 days are between 15 and 18 cm (D-PAF orbits for ERS-1 phases C, E, and F), 10 and 14 cm (JGM 3 orbits for ERS-1 phases C, E, and F; D-PAF orbits for ERS-1 phase G and ERS-2 phase A). Similarly, the T/P-E crossover differences for time lags below 10 days are between 13 and 15 cm (D-PAF orbits for ERS-1 phases C, E, and F) or between 10 and 12 cm (JGM 3 orbits 44 for ERS-1 phases C, E, and F; D-PAF orbits for ERS-1 phase G and ERS-2 phase A). Note that D-PAF orbit accuracy is enhanced for ERS-1 phase G and ERS-2 phase A and is about the same as JGM 3 orbits for ERS-1 phases C, E, and F. This mainly results from an update of the geopotential model (from precise gravity models PGM035 to PGM055) in the D-PAF orbit calculation [*Massmann et al.*, 1997]. Note also that starting from ERS-2 cycle 7, only, satellite laser ranging (SLR) data and Precise Range and Range Rate Experiment (PRARE) data are used as tracking data in the ERS-2 orbit calculation. For the other ERS-1/2 cycles both D-PAF and JGM 3 orbits used SLR and radar altimeter (RA) crossovers as tracking data.

The crossover statistics after adjustment for the two orbits (D-PAF and JGM 3) are almost the same. E-E and T/P-E rms crossover differences are about 6.5 and 7 cm, respectively. They are very similar to T/P-T/P rms crossover differences, which (with the same editing) are about 7 cm rms. T/P-E crossover differences are slightly larger than E-E crossover differences, probably because of the influence of T/P orbit error. Crossover statistics are slightly better with the JGM 3 orbit. The difference in variance is typically 1–2 cm^2. This suggests that the difference in geopotential models between the D-PAF and JGM 3 orbits introduced an additional small high-frequency signal in dual T/P-ERS crossover differences.

The adjusted D-PAF orbit error (i.e., $E(t)$) for ERS-1 phases C, E, and F varies between 9 and 12 cm rms for all processed cycles. The JGM 3 orbit for the same ERS-1 phases is more accurate; its estimated error is between 6 and 9 cm for all processed cycles. D-PAF orbit error for ERS-1 phase G and ERS-2 phase A varies between 6.5 and 9.5 cm, about the same as JGM 3. The rms (SLR plus PRARE) and (SLR plus RA) ERS-2 D-PAF orbit errors are similar. This agrees with results found by *Massmann et al.* [1997].

These estimates provide an independent measure of the accuracy of these ERS-1/2 orbits. They show that good accuracy (7–8 cm) is achieved. Still, these orbit errors are too large

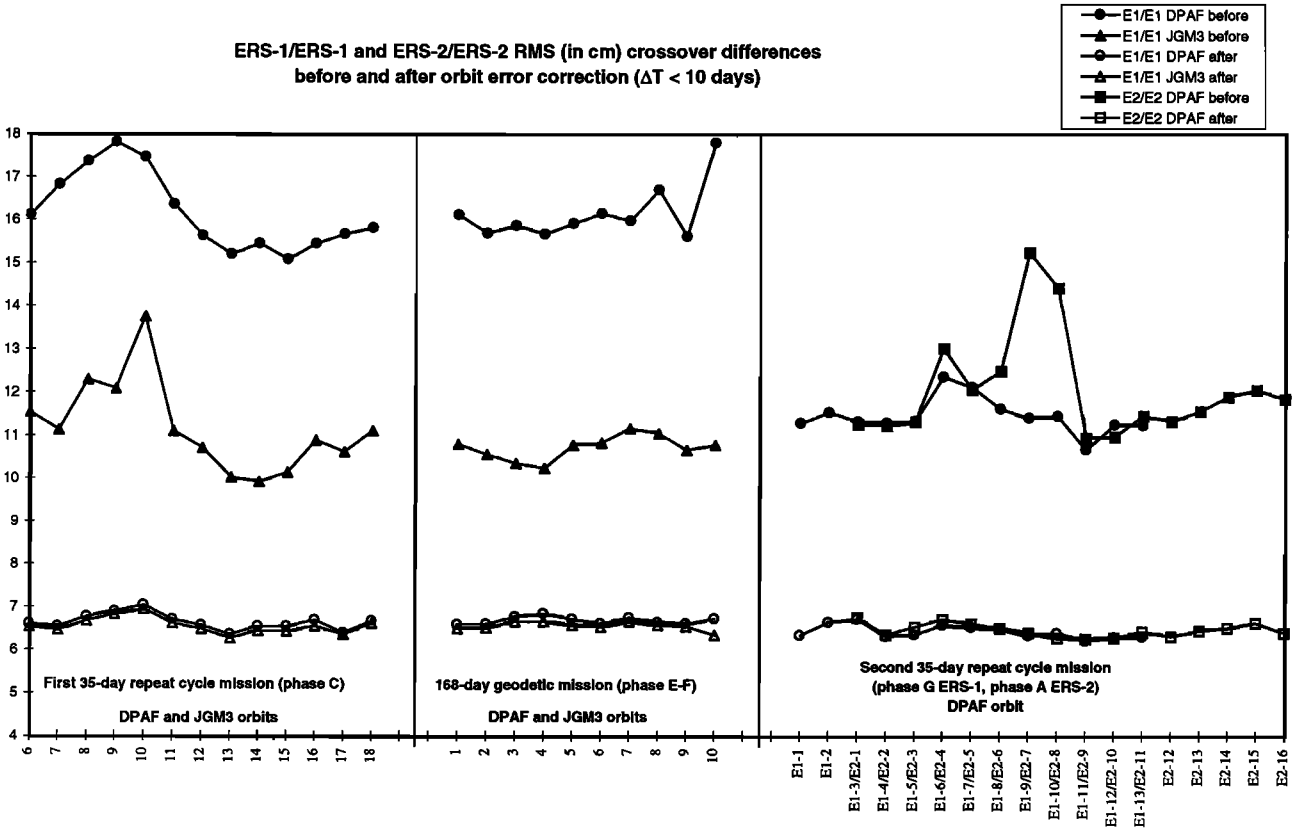

Figure 1. E-E crossover statistics for D-PAF and Joint Gravity Model 3(JGM 3) orbits for ERS-1 cycles 6–18 (phase C, 35 day repeat period), ERS-1 subcycles 1–10 (phases E and F, 168 day repeat period), ERS-1 cycles 1–13 (phase G), and ERS-2 cycles 1–16 (phase A) before and after orbit correction. Units are centimeters.

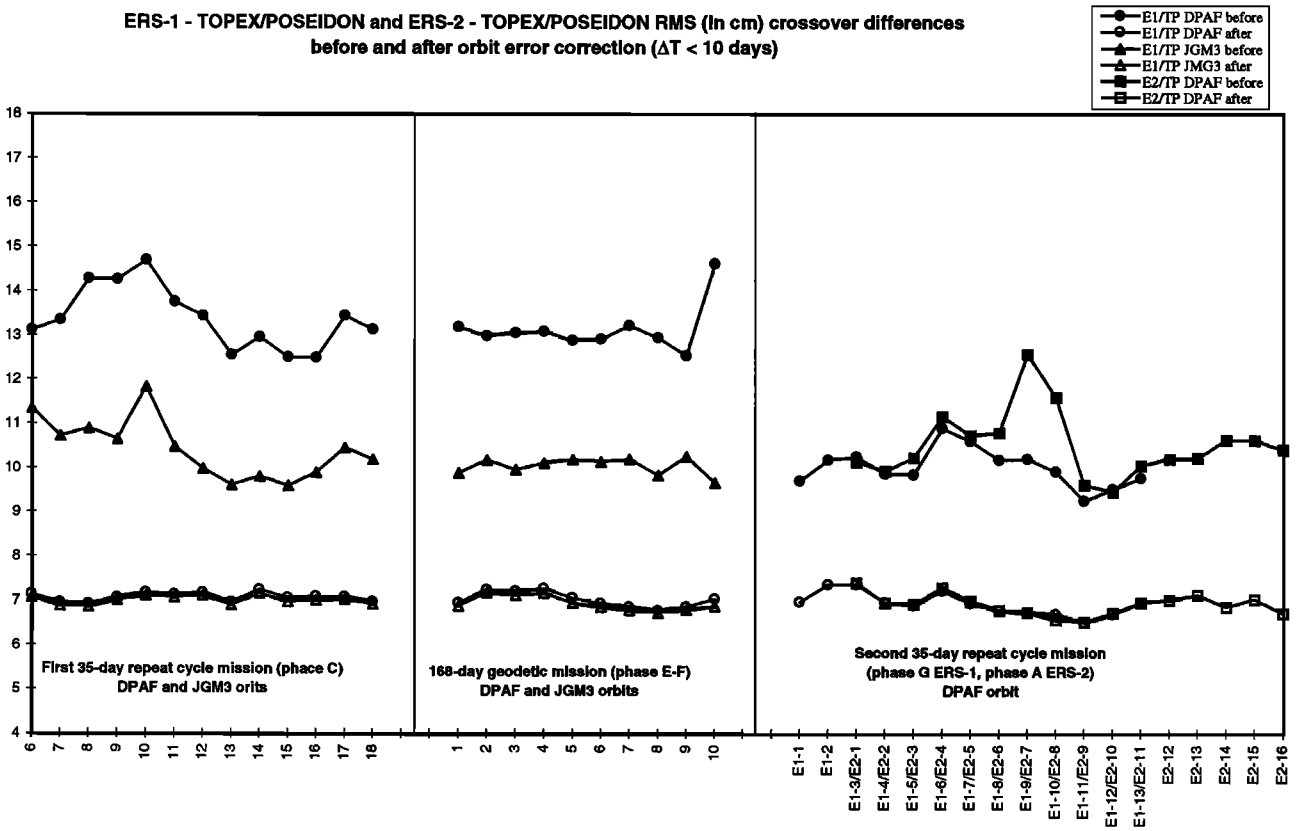

Figure 2. Same as Figure 1 but for T/P-E crossovers. Units are centimeters.

for analyzing the large-scale oceanic signals. The nondynamical adjustment onto T/P is needed to reduce them to a level comparable to T/P orbit error.

4.3. Comparison of D-PAF and JGM 3 Orbits Before and After Orbit Error Correction (ERS-1 Phases C, E, and F)

The comparison of sea surface heights obtained with the D-PAF and JGM 3 orbits (i.e., the difference in orbits) for ERS-1 cycles 6–18 gives a mean rms difference of 11 cm. About half of the difference is constant over time and corresponds to the difference in geographically correlated orbit errors between the D-PAF and JGM 3 orbits (Plate 2a). The variable part of the difference has an rms difference of 8 cm rms (Plate 3a). After orbit error correction the rms difference is only 1.2 cm. About half of the difference between the two corrected solutions is constant over time and is mainly concentrated in equatorial regions (Plate 2b). This probably corresponds to the difference in high-frequency geographically correlated D-PAF and JGM 3 orbit errors which cannot be removed with the spline representation used. This is exemplified on Plate 4, which shows the difference between the two orbits along a given track and the difference between the two orbit error corrections. While the adjustment removes all the long wavelength differences between the two orbits, it cannot remove high-frequency signals which have, in this example, wavelengths shorter than 5000 km. To remove the high-frequency geographically correlated orbit, far more spline knots would be needed. This actually could be achieved by adjusting ERS-1/2 mean profile onto T/P mean profile. In this case the noise at crossovers would be much smaller (because of averaging), and more knots could be added without increasing the adjustment error.

The variable part of the difference (Plate 3b) has a mean rms of 0.7 cm only. The rms is less than 0.5 cm in most areas and reaches 2 cm at high latitudes and in the eastern Mediterranean. It is consistent with the formal error estimates shown in Plate 1b. Note that sea level anomaly is only affected by the variable part of the orbit error. The corrected sea level anomaly for D-PAF and JGM 3 will thus be identical at the centimeter level.

This comparison thus shows that the method is almost insensitive to the initial orbit used because of the very high constraint of the fit. It also confirms the 2 cm precision of the adjustment.

4.4. Influence of T/P Orbit Error

Given the very low T/P orbit error, the estimation of the ERS-1/2 orbit error should not be sensitive to it. T/P JGM 3 orbit error is about 2 cm, and this is not the main source of error in T/P-E crossover differences. Tests were performed using the two available T/P orbits (NASA JGM 3 orbits and CNES JGM 3 estimation by empirical smoothing and filtering (ELFE) orbits). They agree to within about 1.5 cm rms. The influence of these orbits on the ERS orbit error correction is, however, always below 0.5 cm. This means that T/P orbit error is partly filtered out by our method. Of course, the very low frequency part (e.g., frequencies lower than 10 days^{-1}) of the T/P orbit error will directly impact the ERS orbit error estimation and will induce biases on the ERS orbit error. However, the low-frequency part of the JGM 3 T/P orbit error is small [*Marshall et al.*, 1995] and certainly much smaller than the corresponding ERS-1/2 orbit errors.

5. Sea Level Variability

Repeat-track analysis was performed for ERS-1 cycles 6–18 both for D-PAF and JGM 3 orbits. The rms sea level variabilities before orbit error correction for D-PAF and JGM 3 orbits and after orbit error correction for JGM 3 are shown on Plates 5a, 5b, and 6a, respectively. The result with the corrected D-PAF orbit (not shown) is, as expected, almost identical to Plate 6a. Signals in Plates 5a and to a lesser extent 5b are still dominated by orbit error, especially in low-energy areas. The mean difference in sea level variance before and after orbit error correction is 34 cm^2 (D-PAF orbit) and 17 cm^2 (JGM 3 orbit). The rms sea level variability computed from T/P data (Plate 6b) over the same period is in excellent agreement with the ERS-1 corrected sea level variability (Plate 6a). The difference in noise between the T/P and ERS-1 missions explains the slightly larger signals given by ERS-1 in low eddy energy. In high eddy energy (e.g., Gulf Stream) the signals given by ERS-1 are actually smaller. The difference in variance (not shown) is about 40 cm^2, i.e., about 5% of the signal variance. This is because the mean, which is calculated with 3.5 times fewer cycles than T/P, has absorbed a small part of the oceanic signal. As a result, the mean global difference in variance between the ERS-1 and T/P maps is slightly negative (-2 cm^2).

These results show that the ERS-1 data have to be corrected for orbit error to map the oceanic signal. This is shown in Plates 7a and 7b, the mid-November 1992 maps of sea level anomaly obtained with the JGM 3 orbit and the corrected JGM 3 orbit. The maps were obtained with a global suboptimal space-time objective analysis method. The enhancement of ERS-1 data accuracy using T/P as a reference is plain to see. A similar map was obtained using T/P data. The map (Plate 7c) shows that the large-scale features are in excellent agreement with the ERS-1 map. In particular, the large-scale steric effects related to the heating/cooling of surface waters, which are the most difficult signal to preserve in conventional orbit error removal schemes [e.g., *Tai*, 1991], are completely preserved. The differences at smaller scales mainly represent the different space and time sampling of the two satellites. This shows that the T/P and ERS-1/2 data sets are much more consistent after orbit error correction and that they can be merged in the analyses.

6. Conclusion

Formal error estimates and crossover and repeat-track analyses demonstrate that ERS-1/2 orbit error can be estimated to within about 2 cm rms using T/P as a reference. This is comparable to T/P orbit accuracy. The adjustment will also remove any long wavelength error in ERS-1/2 data (e.g., altimeter bias and drift, USO drift, large-scale error in ionospheric correction) which is necessary to obtain consistent T/P and ERS-1/2 data sets. It is also shown that ERS-1/2 orbit error must be corrected before analyzing large-scale oceanic signals and combining ERS-1/2 with T/P data.

The method will be applied on an operational basis to ERS-2 data when they are produced by CERSAT. Corresponding data sets (corrected sea surface heights and sea level anomalies files) will be distributed to the scientific community by AVISO [*AVISO*, 1996b, 1997]. These consistent, homogeneous T/P, ERS-1, and ERS-2 data sets will then be merged using the mapping method described by *Le Traon et al.* [1998] to analyze the sea level variability with a high resolution and a high accuracy.

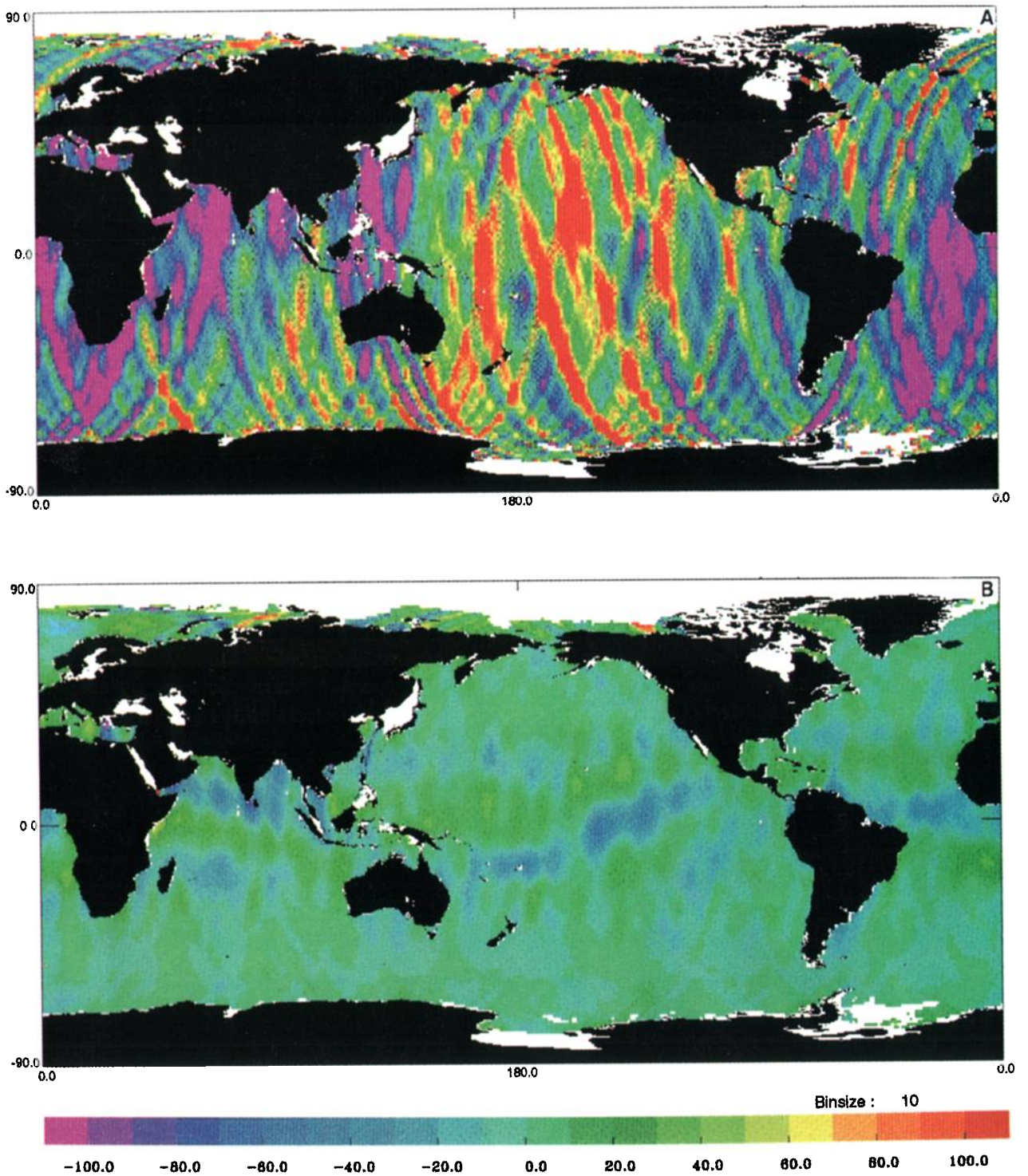

Plate 2. Mean difference (ERS-1 cycles 6–18) in corrected sea surface heights for D-PAF and JGM 3 orbits (a) before and (b) after orbit error reduction.

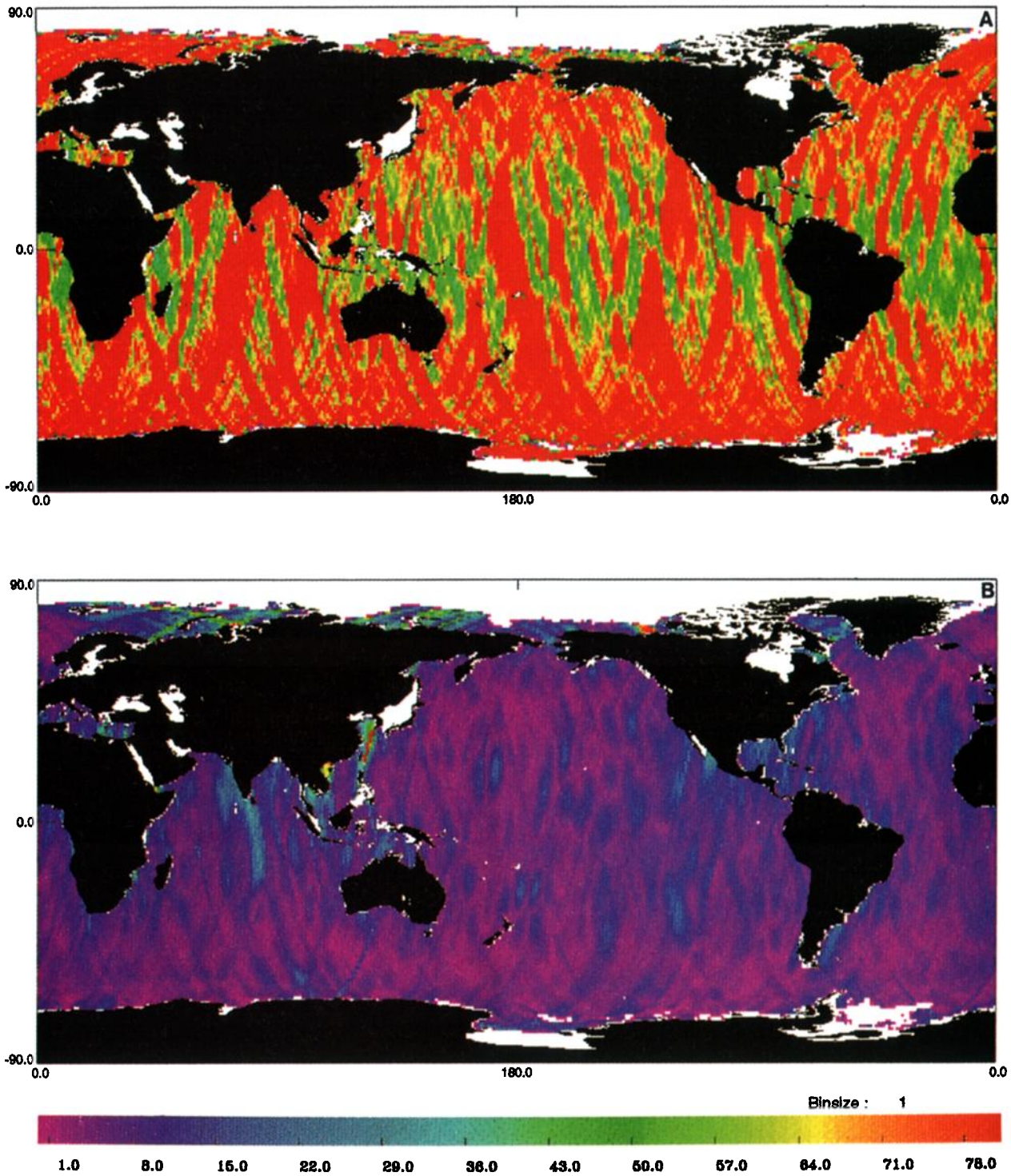

Plate 3. Standard deviation of the difference (ERS-1 cycles 6–18) in corrected sea surface heights between D-PAF and JGM 3 (a) before and (b) after orbit error reduction.

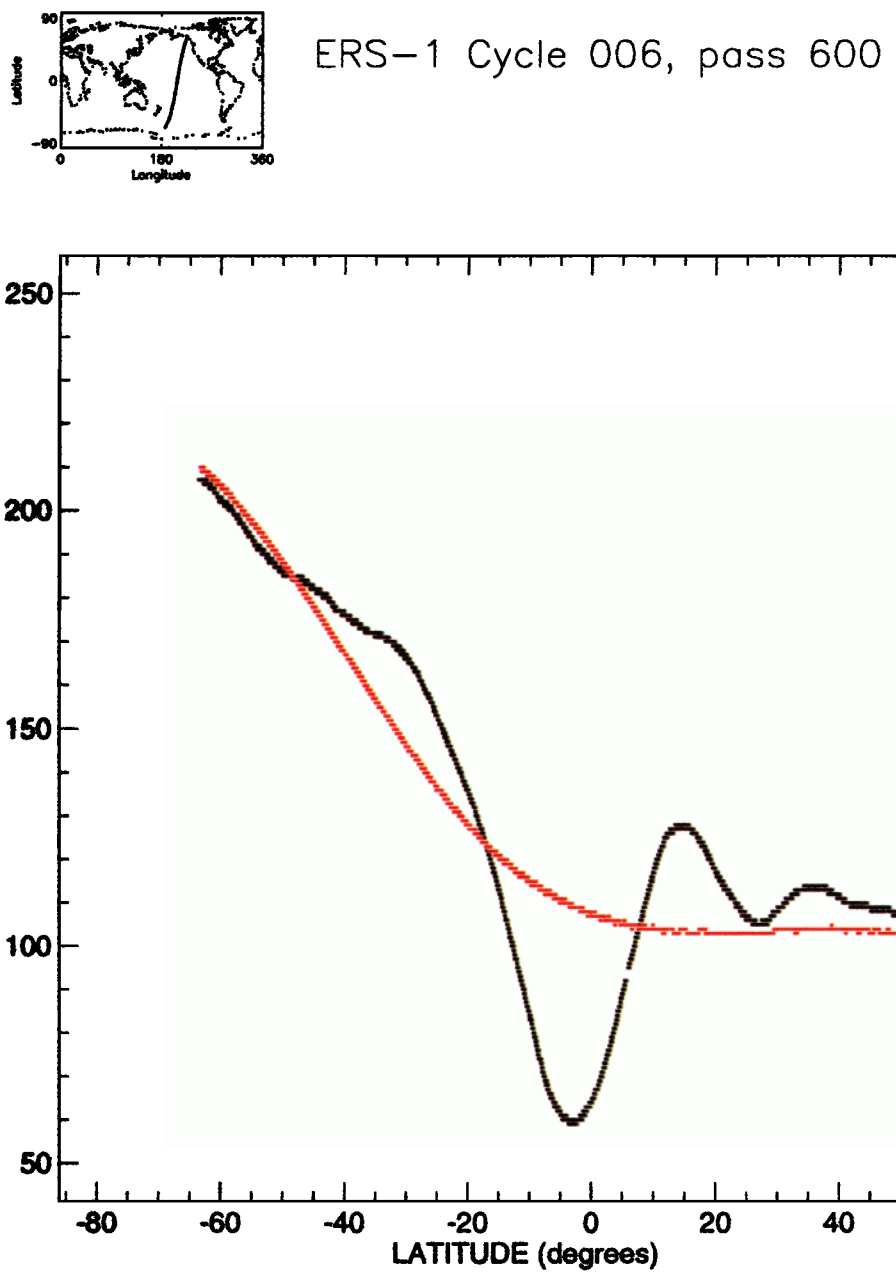

Plate 4. Difference between D-PAF and JGM 3 orbits along ERS-1 track 600 and difference between the D-PAF and JGM 3 orbit error corrections. Units are millimeters.

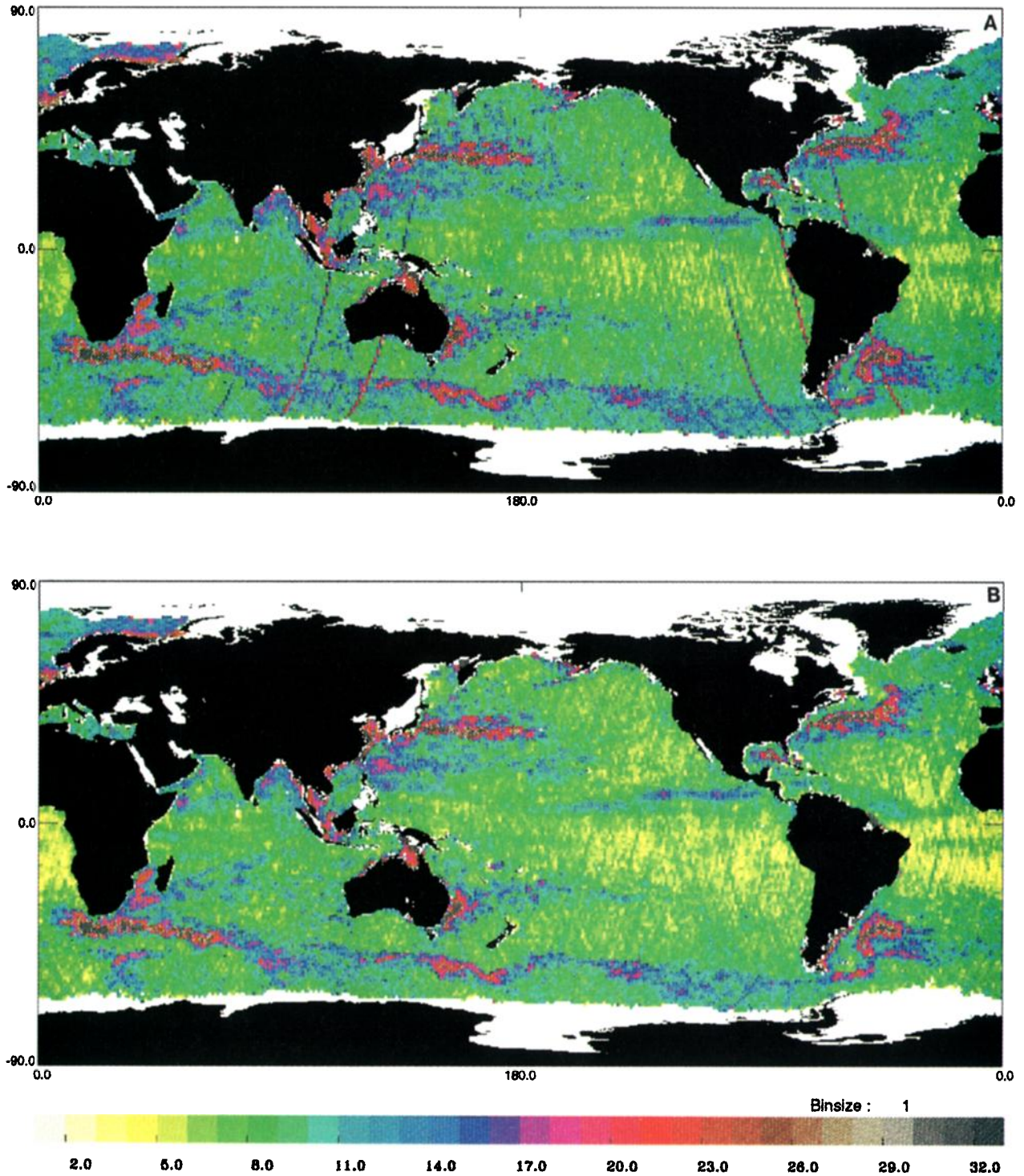

Plate 5. The root-mean-square (rms) sea level variability for ERS-1 cycles 6–18 before orbit error correction for (a) D-PAF and (b) JGM 3 orbits. In centimeters.

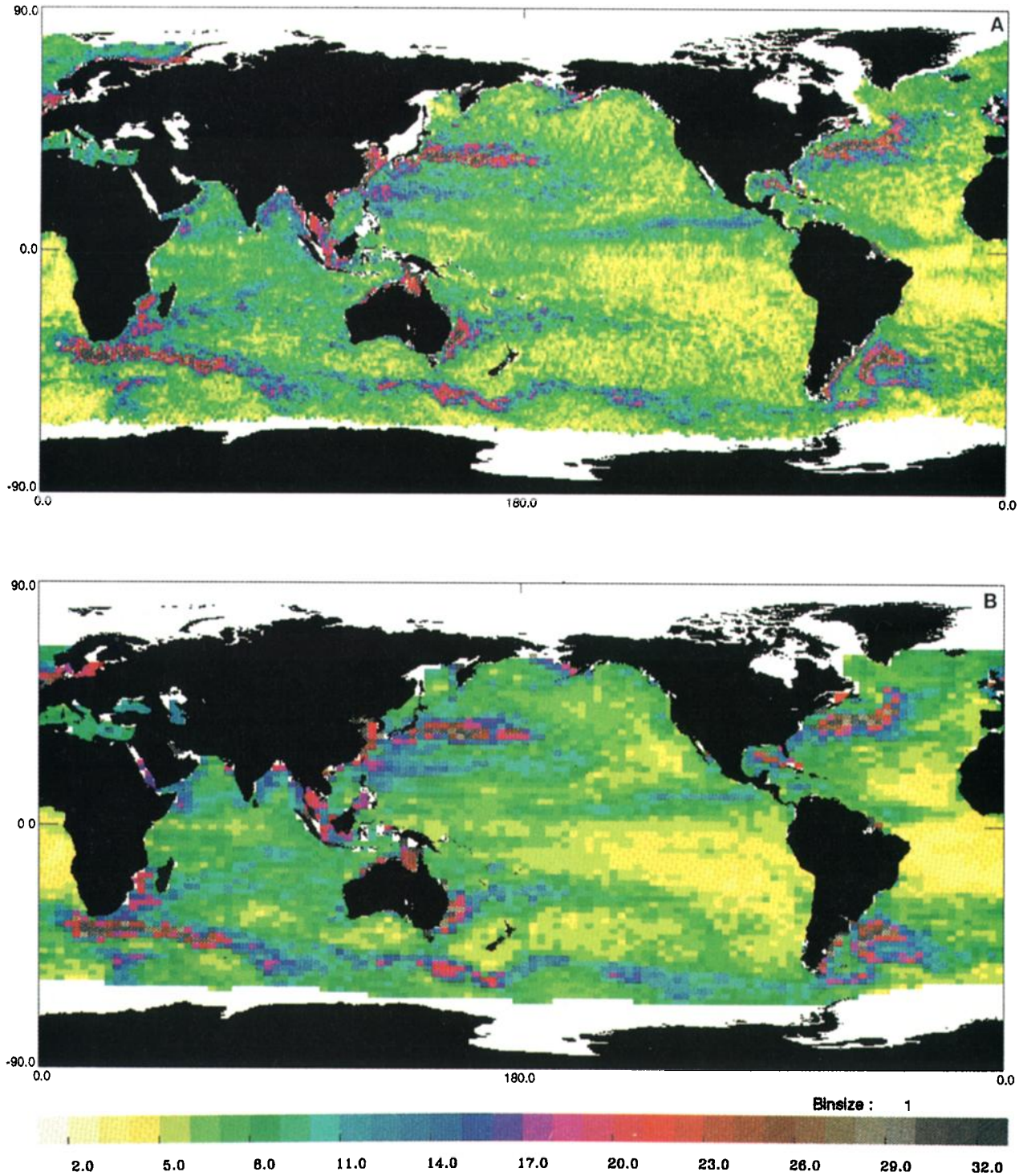

Plate 6. (a) The rms sea level variability for ERS-1 cycles 6–18 after orbit error correction. (b) The rms sea level variability for TOPEX/POSEIDON over the period corresponding to ERS-1 cycles 6–18 (October 1992 to December 1993). In centimeters.

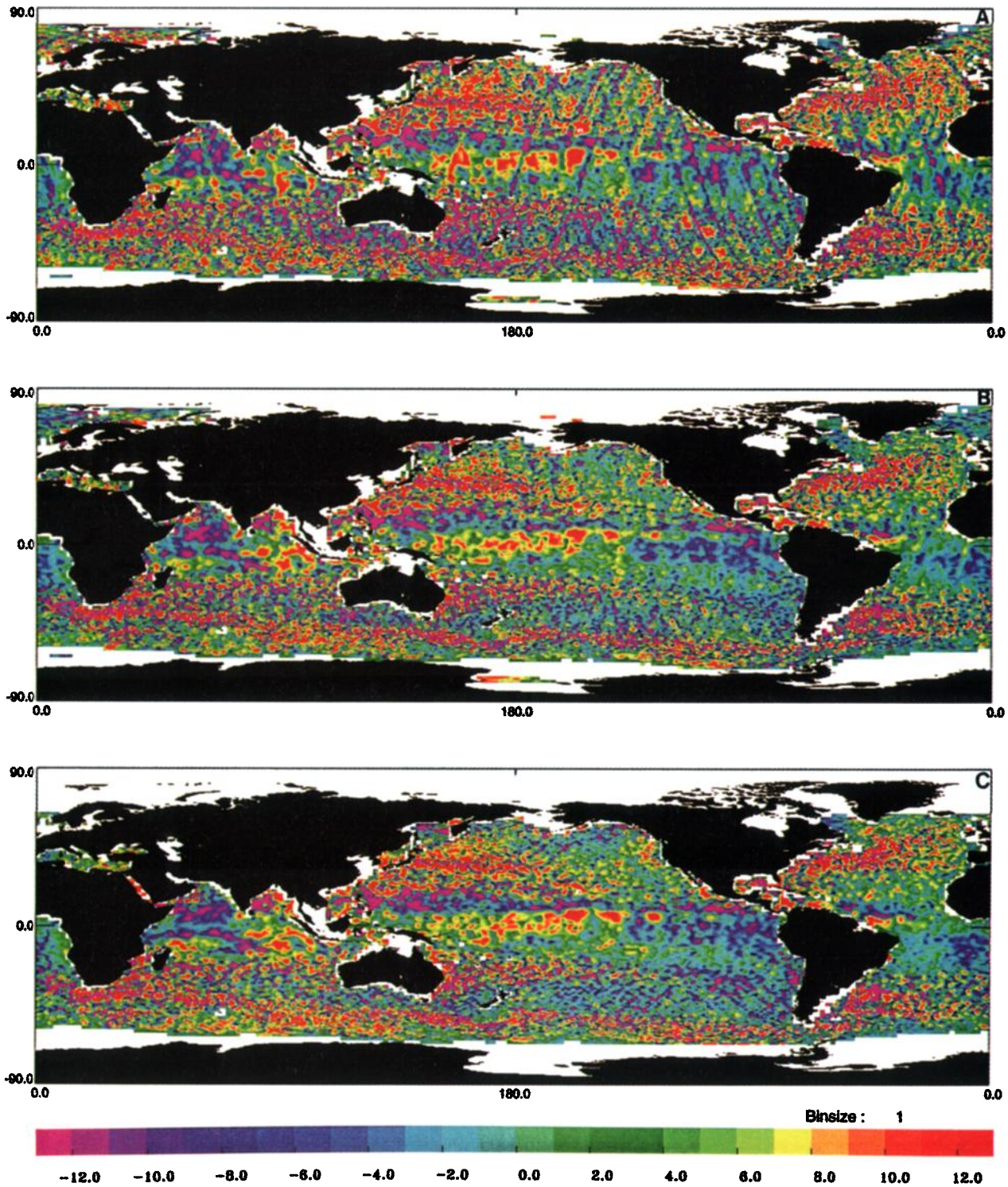

Plate 7. Map of ERS-1 sea level anomaly obtained using (a) the JGM 3 orbit and (b) the corrected JGM 3 orbit for mid-November 1992. (c) Map of T/P sea level anomaly for mid-November 1992. In centimeters.

Acknowledgments. JGM 3 ERS-1 orbits were kindly provided to us by Remko Scharroo from Delft University. The study was supported by the Midi-Pyrénées region, the Environment and Climate AGORA project of the European Union and the French Space Agency (CNES). This work is part of the ESA proposal AO2.F105 "Joint analysis of ERS-1, ERS-2 and TOPEX/POSEIDON altimeter data for oceanic circulation studies."

References

Archiving, Validation, and Interpretation of Satellite Oceanographic Data, AVISO handbook for merged TOPEX/POSEIDON products, 3rd ed., *Handb. AVI-NT-02-101-CN*, Toulouse, France, 1996a.

Archiving, Validation, and Interpretation of Satellite Oceanographic Data, AVISO user handbook corrected sea surface height (CORSSH), 2nd ed., *Handb. AVI-NT-011-311-CN*, Toulouse, France, 1996b.

Archiving, Validation, and Interpretation of Satellite Oceanographic Data, AVISO user handbook: Sea level anomalies (SLA), 2nd ed., *Handb. AVI-NT-011-312-CN*, Toulouse, France, 1997.

Barotto, B., and J. P. Berthias, First results of reduced dynamics with DORIS on TOPEX/POSEIDON and SPOT, *J. Guidance Control*, in press, 1998.

Carnochan, S., P. Moore, and S. Ehlers, ERS-1 radial positioning refinement by dual crossover analysis with TOPEX/POSEIDON, *Adv. Space Res.*, *16*, 119–122, 1995.

Cartwright, D. E., and R. J. Tayler, New computations of the tide-generating potential, *Geophys. J. R. Astron. Soc.*, *33*, 253–264, 1971.

Centre ERS d'Archivage et de Traitement, ERS-1 altimeter products user manual, *Handb. C1-EX-MUT-A21-01-CN*, Brest, France, 1994.

Centre ERS d'Archivage et de Traitement, Altimeter and microwave radiometer ERS products user manual, *Handb. C2-MUT-A-01-IF*, Brest, France, 1996.

Collecte, Localisation, Satellites, Quality assessment of CERSAT altimeter products, *Rep. CLS.OC/NT/93.005*, Agne, France, 1992.

Collecte, Localisation, Satellites, Validation of ERS-1/2 OPR cycles (ERS-1), *Rep. CLS.OC/NT/96.010*, Agne, France, 1996a.

Collecte, Localisation, Satellites, Validation of ERS-1/2 OPR cycles (ERS-2), *Rep. CLS.OC/NT/96.011*, Agne, France, 1996b.

Eanes, R. J., and S. V. Bettadpur, The CSR 3.0 Global Ocean Tide Model, *Rep. CSR-TM-95-06*, Cent. for Space Res., Univ. of Texas, Austin, 1995.

Fu, L.-L., E. J. Christensen, C. A. Yamarone Jr., M. Lefebvre, Y. Menard, M. Dorrer, and P. Escudier, TOPEX/POSEIDON mission overview, *J. Geophys. Res.*, *99*, 24,369–24,381, 1994.

Gaspar, P., and F. Ogor, Estimation and analysis of the sea state bias of the ERS-1 altimeter, technical report of IFREMER contract 94/2.426016/C, Inst. Fr. de Rech. pour l'Exploit. de la Mer, Brest, France, 1994.

Gaspar, P., and F. Ogor, Estimation and analysis of the sea state bias of the new ERS-1 and ERS-2 altimetric data (OPR version 6), *Tech. Rep. CLS/DOS/NT/96.041*, Collect., Localisation, Satell., Agne, France, 1996.

Gaspar, P., F. Ogor, P. Y. Le Traon, and O. Z. Zanife, Estimating the sea state bias of the TOPEX and POSEIDON altimeters from crossover differences *J. Geophys. Res.*, *99*, 24,981–24,994, 1994.

Hayes, J. G., Numerical methods for curve and surface fitting, *Bull. Inst. Math. Appl.*, *10*, 144–152, 1974.

Hernandez, F., P. Y. Le Traon, and R. Morrow, Mapping mesoscale variability of the Azores Current using TOPEX/POSEIDON and ERS-1 altimetry, together with hydrographic and Lagrangian measurements, *J. Geophys. Res.*, *100*, 24,995–25,006, 1995.

Le Traon, P. Y., P. Gaspar, F. Bouyssel, and H. Makhmaraa, Use of TOPEX/POSEIDON data to enhance ERS-1 data, *J. Atmos. Oceanic Technol.*, *12*, 161–170, 1995a.

Le Traon, P. Y., P. Gaspar, F. Ogor, and J. Dorandeu, Satellites work in tandem to improve accuracy of data, *Eos Trans. AGU*, *76*(39), 385, 389, 1995b.

Le Traon, P. Y., F. Nadal, and N. Ducet, An improved mapping method of multiple satellite altimeter data, *J. Atmos. Oceanic Technol.*, in press, 1998.

Marshall, J. A., N. P. Zelensky, S. M. Klosko, D. S. Chinn, S. B. Luthcke, K. E. Rachlin, and R. G. Williamson, The temporal and spatial characteristics of TOPEX/POSEIDON radial orbit error, *J. Geophys. Res.*, *100*, 25,331–25,352, 1995.

Massmann, F. H., K. H. Neumayer, J. C. Raimondo, K. Enninghorst, and H. Li, Quality of the D-PAF orbit before and after the inclusion of PRARE data, paper presented at 3rd ERS Symposium, Eur. Space Agency, Florence, Italy, March 17–21, 1997.

Rapp, R. H., Y. Yi, and Y. M. Wang, Mean sea surface and geoid gradient comparisons with TOPEX altimeter data, *J. Geophys. Res.*, *99*, 24,657–24,667, 1994.

Scharroo, R., K. F. Wakker, and G. J. Mets, The orbit determination accuracy of the ERS-1 mission, in *Proceedings of the Second ERS-1 Symposium—Space at the Service of our Environment, Hamburg, Germany, 11–14 October 1993*, *Eur. Space Agency Spec. Publ., ESA SP-361*, 735–740, 1994.

Tai, C. K., How to observe the gyre to global-scale variability in satellite altimetry: Signal attenuation by orbit error removal, *J. Atmos. Oceanic. Technol.*, *8*, 271–288, 1991.

Tapley, B. D., et al., The Joint Gravity Model 3, *J. Geophys. Res.*, *101*, 28,029–28,049, 1996.

P.-Y. Le Traon and F. Ogor, CLS Space Oceanography Division, 8-10 rue Hermes, Parc Technologique du Canal, 31526 Ramonville Saint-Agne, France. (e-mail: letraon@cls.cnes.fr; ogor@cls.cnes.fr)

(Received November 22, 1996; revised June 12, 1997; accepted July 3, 1997.)